Preprints of the 21st IFAC World Congress (Virtual)
Berlin, Germany, July 12-17, 2020

Feasibility Analysis of Positioning and Navigation Strategies for Railway and Tramway Applications ⋆

Daniela Selvi * **Enrico Meli** * **Benedetto Allotta** *
Andrea Rindi * **Alessandro Capuozzo** ** **Luigi Rucher** **

* *Dipartimento di Ingegneria Industriale (DIEF), Università degli Studi di Firenze, Via di Santa Marta 3, 50139 Firenze, Italy (e-mail: {daniela.selvi,enrico.meli,benedetto.allotta,andrea.rindi}@unifi.it).*
** *Thales Italia S.p.A., Via Provinciale Lucchese 33, 50019 Sesto Fiorentino (Firenze), Italy (e-mail: {alessandro.capuozzo,luigi.rucher}@thalesgroup.com)*

Abstract: The problem of vehicle autonomous driving currently represents a topic of great interest from both theoretical and practical points of view. Among the challenging tasks to be addressed within any autonomous driving framework, one of the most important ones is localization from data collected in real time. Within such framework, this paper is specifically focused on the localization problem for rail vehicles, such as railway and tramway vehicles. Our specific interest is on investigating solutions to the localization problem which are (as much as possible) independent on ground sensor infrastructure and are therefore suitable to be employed on any rail vehicle, irrespective of the ground equipment of the specific tracks. To this end, we refer to a multi-sensor framework and, specifically, to a sensor fusion scheme which collects data from different sensors installed on the vehicle (namely, an Inertial Measurement Unit and a Global Positioning System) and carries out a Kalman-based filtering recursion which relies on a simplified vehicle model. With the aim of identifying a solution for the localization problem providing desirable performance, we carry out a comparative simulation analysis concerning different Kalman-based data fusion strategies (in particular, the Extended Kalman Filter and the Unscented Kalman Filter are considered).

Keywords: Localization, Modeling and simulation of transportation systems, Navigation, Kalman filtering, Tramway vehicles, Railway vehicles

1. INTRODUCTION

The problem of vehicle autonomous driving currently represents a topic of great interest from both theoretical and practical points of view. The increasing attention towards this subject is witnessed by the large number of different applications and studies that have been carried out, involving many research fields such as, for example, signal processing, information fusion, control, and optimization (see for example Meng et al. [2017], Hansen et al. [2016, 2017], Liu et al. [2010], Paden et al. [2016], Li and Leung [2003], Allotta et al. [2002], Malvezzi et al. [2014], Allotta et al. [2014], Lim et al. [2018], Lu et al. [2019]).

Among the challenging tasks to be addressed within any autonomous driving framework, one of the most important ones is *localization* from data collected in real time.

With this respect, many research works have highlighted possibilities and drawbacks associated to solutions based on different sensor types. Specifically, the Global Positioning System (GPS) is very commonly used and can provide satisfactory performance in some operating conditions; however, the reliability of a GPS-based localization system is highly affected by different satellites coming in and out of view, or by interference caused by obstructions, such as the presence of tunnels. Another possible solution is based on inertial navigation systems, which can provide information about position, velocity, and attitude, but such measurements are usually affected by drifts. Solutions based on different sensors, such as, for example, radio detection and ranging (radar), light detection and ranging (LiDAR), cameras, as well as on a fusion of on-board and off-board sensor data, have been proposed; however, the cost associated with such sensors (also in terms of installation and maintenance) has to be taken into account. An interesting comparative survey, highlighting potentials and drawbacks of a number of different technologies, is proposed in Kuutti et al. [2018].

This brief overview highlights the importance of solutions to the localization problem able to combine information provided by multiple different sensors: in fact, such solutions have the potential of improving the performance achieved by each single technology, while overcoming its drawbacks.

⋆ This work has been partially supported by Regione Toscana - POR FSE 2014-2020, Grant UNIFI_FSE2017 - through the project "Tram Navigation by means of IMU and GNSS" (TramNav).

Our paper is specifically focused on the localization problem for rail vehicles, such as railway and tramway vehicles. Even if railway and tramway applications are very different from each other under several aspects (to name a few, maximum reachable velocity, possible presence or not of cars/pedestrians, etc.), they involve a vehicle whose movement is constrained on a rail, which inherently reduces the number of degrees of freedom. In such a context, from wheel odometry it is possible to get a measure of the distance travelled along the track with respect to a specific (starting) point; therefore, this strategy naturally accounts for such a reduced-dimensional space. On the other hand, it has to be mentioned that wheel odometry can be quite an invasive solution (a certain number of sensors are usually installed, each one on a different wheelset), and that the information that is able to provide is reliable only in absence of sliding during acceleration and braking (see for example Malvezzi et al. [2014], Allotta et al. [2012]). Due to such issues, the framework proposed in our paper does not rely on wheel odometry.

Further, our specific interest is on investigating solutions to the localization problem which are as much as possible independent on ground sensor infrastructure, i.e., we aim at obtaining a navigation system which does not rely on balises/tags and is therefore suitable to be employed on any rail vehicle irrespective of the ground equipment of the specific tracks. This would also reduce installation and maintenance costs. Localization strategies which heavily rely on ground sensor infrastructure have been developed and are currently used for example in subway applications (see for example Zhou et al. [2020], Chen et al. [2013], Temple et al. [2017]); however, in the context of railway and tramway positioning, alternative solutions employing different technologies would be preferable. In view of the considerations reported above, we will refer to a multi-sensor framework and, specifically, to a sensor fusion scheme which collects data from different sensors installed on the vehicle and carries out a Kalman-based filtering recursion relying on a simplified vehicle model. Some research work has recently addressed a Kalman-based framework for rail applications (see for example Veillard et al. [2016], Faruqi et al. [2018], Lim et al. [2018]). However, defining a solution which ensures simplicity of implementation (with specific reference to the real-time application of interest) and satisfactory performance while requiring nor high-cost on-board sensors neither consistent and invasive ground sensor infrastructure, is still an open and challenging problem. In the proposed feasibility analysis, we drastically assume that no ground sensors are available, and that measurements are provided by an Inertial Measurement Unit (IMU) and a GPS. The adopted sensor fusion framework exploits the rail constraint within the filtering recursion through a simple model expressing the movement of the vehicle along the rail. With the aim of identifying a solution for the localization problem providing desirable performance, we carry out a comparative simulation analysis concerning different Kalman-based strategies; in particular, the Extended Kalman Filter (EKF) and the Unscented Kalman Filter (UKF) will be considered.

The paper is organized as follows. In Section 2, the overall architecture of an autonomous driving rail vehicle system is presented; further, the models to be used within the filtering recursion are derived. Section 3 briefly recalls the estimation algorithms that are considered in this paper within the sensor fusion framework. A comparative simulation analysis is presented in Section 4, while concluding remarks are provided in Section 5.

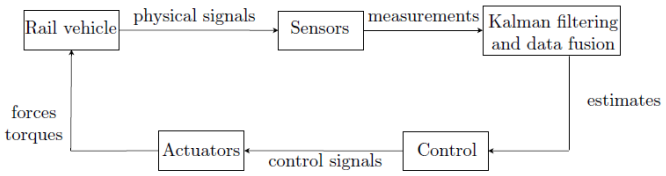

Fig. 1. Autonomous driving for rail vehicles: general architecture

2. PROBLEM SETTING

2.1 Rail-vehicle autonomous driving: general architecture

Vehicle autonomous driving requires to simultaneously address different tasks. The general aim is to make the driving system able to interact with the environment within which it operates with guaranteed performance and safety levels, i.e., collect measurements through sensors, extract useful information, and appropriately react through suitable control actions (a schematic representation is given in Fig. 1). With this respect, the first issue that needs to be addressed is to localize the vehicle at each time with sufficiently high accuracy; then, suitable control strategies can be applied in order to realize vehicle autonomous driving in accordance with prescribed position and speed constraints. The focus of this paper is on the *Kalman filtering and data fusion* task; specifically, within our investigation, the aim is to use measurements in order to provide estimates of specific signals of interest. As it will be clarified in Section 4, in this paper we propose results obtained through a simulation analysis. Specifically, the rail vehicle moving along the track is simulated in Simpack Rail (Multi-Body Simulation SIMPACK MBS Software, Dassault Systèmes) and data are collected emulating IMU and GPS acquisitions to be used within the considered filtering algorithms.

2.2 System and sensor models

The specific objective of this paper is to investigate possible solutions to the localization problem of rail vehicles making use of Kalman-based filtering strategies (such as the EKF and the UKF). The analysis will be concerned on sensor fusion strategies able to use data provided by different sensors to derive, at each time instant, the vehicle location along the track with high accuracy level. In this performance assessment analysis, the model to be used within the estimation procedure will be derived under the assumption that the slope variations of the track are negligible so that the vehicle motion can be well described through a two-dimensional framework. We point out that this simplifying assumption is only considered for model derivation, whereas our feasibility analysis is also directed to more general situations (see Section 4).

We consider an IMU and a GPS, rigidly fixed on the vehicle, acquiring measurements with sampling inter-

vals $T_{s,IMU}$ and $T_{s,GPS}$, respectively. We assume that $T_{s,GPS} = K\,T_{s,IMU}$, with K a positive integer, and that measurement acquisitions from the GPS occur synchronously with those from the IMU; this assumption is made for simplicity, but could be removed by accounting for time stamps and aligning data to a common time frame before processing them. We assume that all the measurements are provided with respect to the same inertial coordinate system; as we restrict the analysis to a two-dimensional frame, we will denote such coordinate system by Oxy (see Fig. 2). This assumption simplifies the overall framework without any loss of generality in the sense that, if some measurements are provided with respect to a different coordinate system, then it is sufficient to introduce appropriate rotation matrices in order to express all data with respect to the same frame of reference.

Specifically, we use the noisy measurements provided by IMU and GPS as follows. Let $t = 0, 1, \cdots$, denote discrete time instants, i.e., $t = \kappa T_s$, with κ a non-negative integer, and $T_s = T_{s,IMU}$. The IMU, located in the point $p_{IMU}(t) = [p_{IMU,x}(t),\, p_{IMU,y}(t)]^\top$ (rigidly connected to the vehicle), provides angular velocity and linear acceleration measurements; further, we assume that an estimate of the orientation of the IMU with respect to the inertial frame Oxy is also available. Therefore, in the considered two-dimensional framework, the following measurements are available:

- the angular velocity
$$\omega^{\text{meas}}_{IMU}(t) = \omega_{IMU}(t) + d^{\omega}_{IMU}(t) \tag{1}$$
around x and y axes, which we can consider as the sum of the corresponding noiseless measurement $\omega_{IMU}(t) = [\omega_{IMU,x}(t),\, \omega_{IMU,y}(t)]^\top$ and a noise $d^{\omega}_{IMU}(t) = [d^{\omega}_{IMU,x}(t),\, d^{\omega}_{IMU,y}(t)]^\top$;
- the linear acceleration
$$a^{\text{meas}}_{IMU}(t) = a_{IMU}(t) + d^{a}_{IMU}(t) \tag{2}$$
along x and y axes, which we can consider as the sum of the noiseless $a_{IMU}(t) = [a_{IMU,x}(t),\, a_{IMU,y}(t)]^\top$ and a noise $d^{a}_{IMU}(t) = [d^{a}_{IMU,x}(t),\, d^{a}_{IMU,y}(t)]^\top$;
- the orientation
$$\varphi^{\text{meas}}_{IMU}(t) = \varphi_{IMU}(t) + d^{\varphi}_{IMU}(t) \tag{3}$$
with respect to the inertial frame Oxy, which we can consider as the sum of the noiseless $\varphi_{IMU}(t) = [\varphi_{IMU,x}(t),\, \varphi_{IMU,y}(t)]^\top$ and a noise $d^{\varphi}_{IMU}(t) = [d^{\varphi}_{IMU,x}(t),\, d^{\varphi}_{IMU,y}(t)]^\top$.

From the GPS measurements we can obtain a noisy evaluation of the position of the GPS receiver
$$p^{\text{meas}}_{GPS}(t) = p_{GPS}(t) + d_{GPS}(t) \tag{4}$$
in the Oxy frame, which we can consider as the sum of the noiseless GPS position $p_{GPS}(t) = [p_{GPS,x}(t),\, p_{GPS,y}(t)]^\top$ (rigidly connected to the vehicle) and a noise $d_{GPS}(t) = [d_{GPS,x}(t),\, d_{GPS,y}(t)]^\top$.

Remark 1. As mentioned above, the GPS collects measurements at acquisition time instants which are synchronous with those of the IMU, but with sampling time $T_{s,GPS} = K\,T_{s,IMU} = K\,T_s$. Nevertheless, we can use the same time frame for both IMU and GPS measurements (and thus the dependence on the same discrete time variable t) with the understanding that GPS measurements are available one out of K IMU acquisition instants.

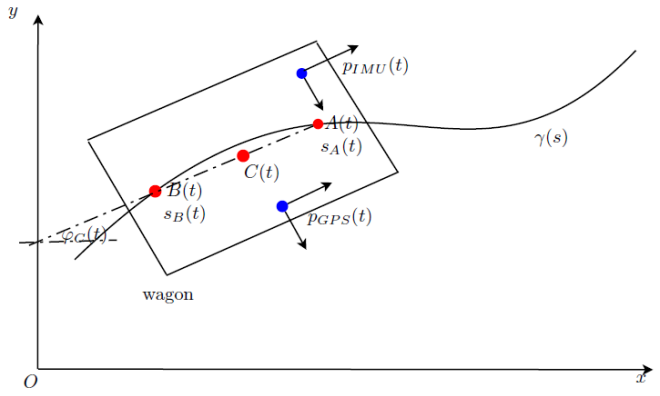

Fig. 2. Simplified framework considered to derive the system and sensor models.

The vehicle, moving along the track, is modelled in discrete time as a nonlinear system
$$\xi(t+1) = f(\xi(t), u(t), d(t))\,, \tag{5}$$
where $\xi(t)$ is the system state (to be estimated), $u(t)$ is the control input, and $d(t)$ represents the process noise. Specifically, we refer to the simplified framework of Fig. 2, which shows a single wagon moving along the curve $\gamma(s(t))$ representing the track and parameterized by the arc-length $s(t)$ travelled with respect to a starting point $s(0)$. We denote by $A(t) = [x_A(t),\, y_A(t)]^\top$ and $B(t) = [x_B(t),\, y_B(t)]^\top$ the contact points between the wagon and the track (for simplicity we consider a single front contact point and a single rear contact point), which are equivalently expressed in terms of arc-length as $s_A(t)$ and $s_B(t)$, respectively. We further consider a point $C(t) = [x_C(t),\, y_C(t)]^\top$ belonging to the wagon and representing the origin of the body frame. The orientation of such frame with respect to the inertial frame Oxy is given by the angle $\varphi_C(t)$.

In order to localize the wagon along the track, we are interested in estimating the time evolution of $s_A(t)$ and $s_B(t)$. From kinematic relations, in the absence of noise we can easily obtain

$$\begin{aligned} s_A(t+1) = s_A(t) + T_s\,\tau(s_A(t))^\top\,[v_{IMU}(t) \\ +\Omega_{IMU}(t) \wedge \mathcal{R}(\varphi_{IMU}(t))A_{IMU}] \end{aligned} \tag{6}$$

$$\begin{aligned} s_B(t+1) = s_B(t) + T_s\,\tau(s_B)^\top\,\{v_{IMU}(t) \\ +\Omega_{IMU}(t) \wedge \mathcal{R}(\varphi_{IMU}(t))A_{IMU} \\ -\ell\,[-sin(\varphi_C(t)),\, cos(\varphi_C(t))]^\top \omega_C(t)\} \end{aligned} \tag{7}$$

where $\wedge$ denotes cross product and

- $\tau(s_A(t))$ is the versor in the xy plane tangent to $\gamma(s)$ in $s_A(t)$;
- $v_{IMU}(t) = [v_{IMU,x}(t),\, v_{IMU,y}(t)]^\top$ is the velocity experienced by the IMU (i.e., the velocity of the point $p_{IMU}(t)$; we recall that $p_{IMU}(t)$ is rigidly connected to the vehicle);
- $\Omega_{IMU}(t) = \omega_{IMU}(t)\,k$, where k is the versor orthogonal to the xy plane, pointing in the direction of the axis forming a right-handed frame with x and y;

- $\mathcal{R}(\varphi_{IMU}(t))$ is the rotation matrix expressing the orientation of the IMU frame of reference with respect to the inertial coordinate system Oxy;
- A_{IMU} is the position of point A expressed in the IMU frame of reference (it can be assumed to be constant over time as the wagon can be considered a rigid body);
- $\tau(s_B(t))$ is the versor in the xy plane tangent to $\gamma(s)$ in $s_B(t)$;
- ℓ is the length of vector $(A-B)$, where A and B are defined in the Oxy coordinate system as $A \doteq (A-O)$ and $B \doteq (B-O)$, respectively;
- $\omega_C(t)$ is the angular velocity expressed in the body frame of reference.

Note however that the noiseless $\omega_{IMU}(t)$ and $\varphi_{IMU}(t)$ are actually unavailable, as the IMU can provide only the corresponding noisy $\omega^{\text{meas}}_{IMU}(t)$ and $\varphi^{\text{meas}}_{IMU}(t)$. Note further that the velocity $v_{IMU}(t)$ can be computed by integrating the available $a^{\text{meas}}_{IMU}(t)$ in (2); however, such an operation introduces non-negligible numerical errors, i.e.,

$$v^{\text{int}}_{IMU}(t+1) = v^{\text{int}}_{IMU}(t) + T_s\, a^{\text{meas}}_{IMU}(t) + d^{\text{int}}_{IMU}(t)\,. \quad (8)$$

As for the GPS, we can express the position of the receiver $p_{GPS}(t)$ in (4) with respect to both $s_A(t)$ and $s_B(t)$ as follows:

$$p_{GPS}(t) = \gamma(s_A(t)) - \mathcal{R}(\varphi_{GPS}(t))A_{GPS} \quad (9)$$

$$p_{GPS}(t) = \gamma(s_B(t)) - \mathcal{R}(\varphi_{GPS}(t))B_{GPS}\,, \quad (10)$$

where:

- $\mathcal{R}(\varphi_{GPS}(t))$ is the rotation matrix expressing the orientation of the GPS frame of reference with respect to the inertial coordinate system Oxy;
- A_{GPS} is the position of point A expressed in the GPS frame of reference (it can be assumed to be constant);
- B_{GPS} is the position of point B expressed in the GPS frame of reference (it can be assumed to be constant).

Note that, in the absence of noise, (9) and (10) return the same result for $p_{GPS}(t)$.

Remark 2. Without loss of generality, we can assume that the IMU, GPS, and body frames of reference have the same orientation with respect to the inertial coordinate system Oxy (this simplifying assumption could be removed by introducing appropriate rotation matrices, for example when it is necessary to take into account orientation misalignments occurring during sensor installation). Accordingly, in the above expressions we have $\varphi_C(t) = \varphi_{GPS}(t) = \varphi_{IMU}(t)$ and $\omega_C(t) = \omega_{IMU}(t)$.

Summing up, by defining

$$\xi(t) = \begin{bmatrix} \xi_1(t) \\ \xi_2(t) \\ \xi_3(t) \\ \xi_4(t) \end{bmatrix} = \begin{bmatrix} s_A(t) \\ s_B(t) \\ v_{IMU,x}(t) \\ v_{IMU,y}(t) \end{bmatrix} \quad (11)$$

$$u = \begin{bmatrix} u_1(t) \\ u_2(t) \\ u_3(t) \\ u_4(t) \end{bmatrix} = \begin{bmatrix} \varphi_{IMU}(t) \\ \omega_{IMU}(t) \\ a_{IMU,x}(t) \\ a_{IMU,y}(t) \end{bmatrix} \quad (12)$$

$$z(t) = p^{\text{meas}}_{GPS}(t) \quad (13)$$

we obtain the following expressions for the system model $\xi(t+1) = f(\xi(t), u(t), d(t))$ and the measurement equation $z(t) = h(\xi(t), u(t), d_z(t))$:

$$\begin{aligned} \xi_1(t+1) = \xi_1(t) + T_s\, \tau(\xi_1(t))^\top \Bigg\{ \begin{bmatrix} \xi_3(t) \\ \xi_4(t) \end{bmatrix} \\ + u_2(t)\, k \wedge \mathcal{R}(u_1(t)) A_{IMU} \Bigg\} + d_1(t) \end{aligned} \quad (14)$$

$$\begin{aligned} \xi_2(t+1) = \xi_2(t) + T_s\, \tau(\xi_2(t))^\top \Bigg\{ \begin{bmatrix} \xi_3(t) \\ \xi_4(t) \end{bmatrix} \\ + u_2(t)\, k \wedge \mathcal{R}(u_1(t)) A_{IMU} \\ - \ell \begin{bmatrix} -sin(u_1(t)) \\ cos(u_1(t)) \end{bmatrix} u_2(t) \Bigg\} + d_2(t) \end{aligned} \quad (15)$$

$$\xi_3(t+1) = \xi_3(t) + T_s u_3(t) + d_3(t) \quad (16)$$

$$\xi_4(t+1) = \xi_4(t) + T_s u_4(t) + d_4(t) \quad (17)$$

$$\begin{aligned} z(t) = \frac{1}{2} \Big[(\gamma(\xi_1(t)) - \mathcal{R}(u_1(t)) A_{GPS}) \\ + (\gamma(\xi_2(t)) - \mathcal{R}(u_1(t)) B_{GPS}) \Big] + d_z(t)\,. \end{aligned} \quad (18)$$

With respect to the model form (5), the process disturbance $d(t)$ appears as an additive term, i.e.,

$$\xi(t+1) = f(\xi(t), u(t)) + d(t)\,,$$

and is defined as $d(t) = [d_1(t),\, d_2(t),\, d_3(t),\, d_4(t)]^\top$ and includes the effects of the noises and numerical errors which have been highlighted in (1) - (3) and (8).

Note that the measurement equation (18) is obtained from (4),(9) and (10) by averaging the information on $p_{GPS}(t)$ provided by the estimate of both $s_A(t)$ and $s_B(t)$. This operation has the objective of providing a better evaluation of the unavailable noiseless $p_{GPS}(t)$. The measurement noise $d_z(t)$ appears as an additive term, i.e.,

$$z(t) = h(\xi(t), u(t)) + d_z(t)\,,$$

and includes the effect of the uncertainties on $p_{GPS}(t)$ and those expressed by $d_{GPS}(t)$ in (4).

In order to employ the derived system and measurement models within a Kalman-based estimation algorithm, we will assume that $d(t) \sim \mathcal{N}(0, Q(t))$ is a zero-mean white Gaussian noise with covariance $Q(t)$; similarly, we will assume that $d_z(t) \sim \mathcal{N}(0, R(t))$ a zero-mean white Gaussian noise with covariance $R(t)$.

3. ESTIMATION ALGORITHMS

The aim of this section is to recall the basic ideas of estimation algorithms which represent candidate strategies for the localization problem of interest. In particular, we will consider the EKF and the UKF. Then, we will employ the system and measurement models derived in Section 2 within such techniques, and will evaluate and compare in simulation the performance obtained by the two algorithms.

Interesting references for the estimation algorithms that will be briefly recalled in the following can be found for example in Bar-Shalom et al. [2001], Julier and Uhlmann [1997, 2004].

3.1 Extended Kalman Filter

The Extended Kalman Filter is quite a commonly used estimation algorithm, especially due to the simplicity of its implementation. The basic idea behind EKF is to linearize, at each iteration, the nonlinear system and measurement functions through Taylor expansion around the current estimate by computing the Jacobians of the nonlinear model function $f(\cdot)$ and measurement function $h(\cdot)$ as follows:

$$A(t) = \left.\frac{\partial f(\cdot)}{\partial \xi}\right|_{\hat{\xi}(t|t),u(t)}, \quad C(t) = \left.\frac{\partial h(\cdot)}{\partial \xi}\right|_{\hat{\xi}(t|t-1),u(t)} \tag{19}$$

This approximations allows one to actually resort to a linear model (for both system and measurement equations), to which standard Kalman filtering can be applied. As well known, the performance achievable by EKF is highly dependent on the discrepancy between the linearized and the actual nonlinear models; in fact, linearization errors are not accounted for within the evaluation of estimate uncertainty (i.e., within the computation of covariance matrices). With this respect, it is also worth mentioning that the initial estimate error affects the algorithm performance; this issue must be considered within the application of interest, with particular reference to the requirement of reducing, as much as possible, ground sensor infrastructure (specifically, appropriately placed tags/balises could be necessary in order to improve the algorithm outcome).

3.2 Unscented Kalman Filter

The Unscented Kalman Filter aims at avoiding any approximation of the nonlinear system and measurement model equations; to this aim, the Unscented Transform is employed. To briefly recall the basic concepts of the Unscented Transform, we consider a generic state η and a generic nonlinear function $g(\cdot)$ such that $\lambda = g(\eta)$. The idea underlining the Unscented Transform is to deterministically select a certain number n_σ of samples η_s, $s = 1, \ldots, n_\sigma$, in the state space so that the overall set describes the most important features of the probability distribution of η. In the case of Gaussian distribution, $n_\sigma = 2n + 1$, where n is the state dimension. A weight w_s is associated to each sample η_s; the pair (η_s, w_s) is referred to as *sigma point*. Each sample η_s is propagated through $g(\cdot)$ to produce "transformed" samples $\lambda_s = g(\eta_s)$, $s = 1, \ldots, 2n+1$, from which it is possible to compute

$$\overline{\lambda} = \sum_{s=1}^{2n+1} w_s \lambda_s \tag{20}$$

$$P_\lambda = \sum_{s=1}^{2n+1} w_s (\lambda_s - \overline{\lambda})(\lambda_s - \overline{\lambda})^\top . \tag{21}$$

Then, the distribution of λ is approximated by a Gaussian with mean $\overline{\lambda}$ and covariance P_λ. With this respect, we recall that a Gaussian distribution is exhaustively known once its mean and covariance are determined. By employing the Unscented Transform, UKF generates sigma points at each iteration and propagates them through the nonlinear system and measurement functions $f(\cdot)$ and $h(\cdot)$, respectively. Therefore, UKF does not require to compute the Jacobian of such nonlinear functions; further, as the number of sigma points depends linearly on the state dimension, the computational burden is quite limited, thus making the UKF algorithm suitable to being adopted for real-time estimation tasks.

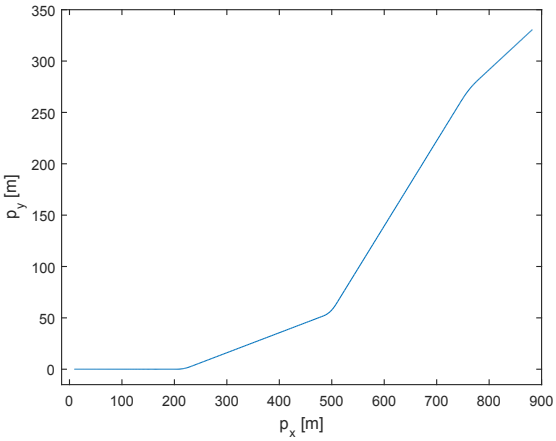

Fig. 3. Rail trajectory considered in the simulation scenario.

4. COMPARATIVE PERFORMANCE EVALUATION

In this section, we address the feasibility analysis of the considered positioning framework when the EKF and UKF algorithms briefly recalled in Section 3, relying on the models described in Section 2, are employed for data fusion. The analysis is carried out through a comparative test in simulation, which is performed in two steps. First, a three-dimensional multibody model of a rail vehicle moving along the track represented in Fig. 3 is simulated in Simpack Rail; this simulation provides noiseless IMU and GPS measurements ω_{IMU}, a_{IMU}, φ_{IMU} (with sampling time $T_s = T_{s,IMU} = 10^{-2}$ s), and p_{GPS} (with sampling time $T_{s,GPS} = 10\,T_s = 10^{-1}$ s), which are then corrupted by zero-mean random noises drawn from Gaussian distributions to obtain $\omega_{IMU}^{\text{meas}}$, a_{IMU}^{meas}, $\varphi_{IMU}^{\text{meas}}$, p_{GPS}^{meas}. With this respect, suitable values for the noise variances are chosen so that such data reasonably emulate real measurements provided by average-performance sensors. Then, the EKF and UKF algorithms, implemented on the basis of the system and measurement models (14)-(18), are run and their performance is evaluated and compared. To this aim, let $\overline{\xi}(t)$ represent the ground truth, i.e., the vector composed of the "true" positions $\overline{s}_A(t)$, $\overline{s}_B(t)$ and velocities $\overline{v}_{IMU,x}(t)$, $\overline{v}_{IMU,y}(t)$ provided by the three-dimensional multibody model of the rail vehicle simulated in Simpack Rail; note that such variables are actually unknown to the algorithms, and are used herein only for performance assessment purpose. We define the estimation error as

$$e(t) = \begin{bmatrix} e_1(t) \\ e_2(t) \\ e_3(t) \\ e_4(t) \end{bmatrix} := \xi(t) - \overline{\xi}(t) = \begin{bmatrix} s_A(t) - \overline{s}_A(t) \\ s_B(t) - \overline{s}_B(t) \\ v_{IMU,x}(t) - \overline{v}_{IMU,x}(t) \\ v_{IMU,y}(t) - \overline{v}_{IMU,y}(t) \end{bmatrix} \tag{22}$$

In the first simulation setup, we assume that the maximum slope along the whole track is 4×10^{-3}. A comparison of the

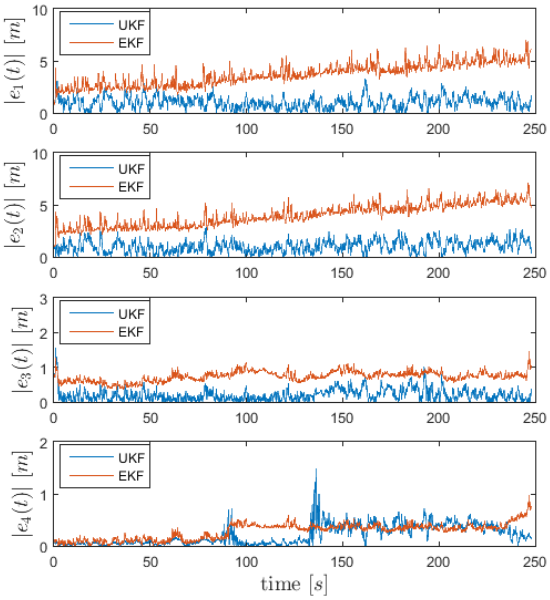

Fig. 4. First test. Comparison between the performances achieved by using UKF and EKF within the considered positioning architecture (from top to bottom: time evolution of $|e_1(t)|$, $|e_2(t)|$, $|e_3(t)|$ and $|e_4(t)|$).

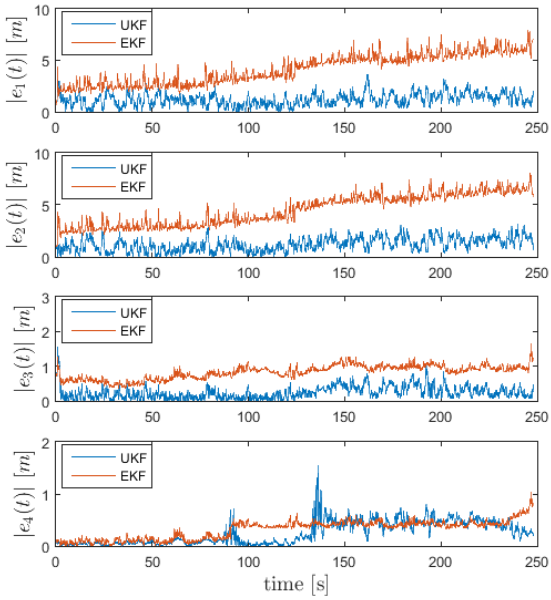

Fig. 5. Second test. Comparison between the performances achieved by using UKF and EKF within the considered positioning architecture (from top to bottom: time evolution of $|e_1(t)|$, $|e_2(t)|$, $|e_3(t)|$ and $|e_4(t)|$).

performance achieved when UKF and EKF, respectively, are used, is reported in Fig. 4 in terms of the absolute value of the estimation error $e(t)$ obtained for the positions $s_A(t)$ and $s_B(t)$ and the velocities $v_{IMU,x}(t)$ and $v_{IMU,y}(t)$. We can note that using UKF within the data fusion strategy provides in general better performance, especially for what concerns the error on positions $s_A(t)$ and $s_B(t)$; in fact, even if the model used within the filters (and described in Section 2) is simple, we note that the nonlinearities in equations (14) and (15) can hardly be accurately approximated by Jacobian computation (i.e., by first-order approximation). In the second simulation test, we assume that the slope in the last $500\,m$ of the track in Fig. 3 is 3×10^{-2}, and show in Fig. 5 a comparison of the performance achieved when UKF and EKF, respectively, are used. The results are comparable to those obtained in the previous test, thus suggesting that the 2D simple model of the rail vehicle derived in Section 2.2 from kinematic relations can be successfully employed within a Kalman-based data fusion even in more general situations. We point out that further tests, not reported here, have been carried out, and that all of them have underlined better accuracy as well as better robustness properties of UKF than EKF with respect to variations in disturbances/noises and algorithm initialization (initial guess and associated initial uncertainty). This preliminary analysis suggests that UKF is a suitable estimation algorithm to be employed within positioning frameworks for tramway and railway applications.

5. CONCLUSION

In this work, the localization problem for rail vehicles, such as tramway and railway vehicles, has been addressed. Our interest has been focused on investigating solutions which are (as much as possible) independent on ground sensor infrastructure; the considered framework relies on a sensor fusion scheme which collects data from an IMU and a GPS installed on the vehicle and carries out a Kalman-based filtering recursion based on a simplified vehicle model. Specifically, the EKF and the UKF algorithms have been considered, and their performance have been compared through a simulation analysis involving a multibody model of a rail vehicle. With this respect, the simulation analysis has underlined that the UKF algorithm is a promising data fusion strategy to be used within the considered localization system. Future investigations will be concerned on analyzing the performance achievable on real-case scenarios, as well as on including different sensors within the positioning framework.

REFERENCES

Allotta, B., Colla, V., and Malvezzi, M. (2002). Train position and speed estimation using wheel velocity measurement. *Proceedings of the Institution of Mechanical Engineers, Part F: Journal of Rail and Rapid Transit*, 216(3), 207–225.

Allotta, B., D'Adamio, P., Malvezzi, M., Pugi, L., Ridolfi, A., Rindi, A., and Vettori, G. (2014). An innovative localisation algorithm for railway vehicles. *Vehicle System Dynamics: International Journal of Vehicle Mechanics and Mobility*, 52(11), 1443–1469.

Allotta, B., Pugi, L., Ridolfi, A., Malvezzi, M., Vettori, G., and Rindi, A. (2012). Evaluation of odometry algorithm performances using a railway vehicle dynamic model. *Vehicle System Dynamics: International Journal of Vehicle Mechanics and Mobility*, 50, 699–724.

Bar-Shalom, Y., Rong Li, X., and Kirubarajan, T. (2001). *Estimation with applications to tracking and navigation:*

Theory Algorithms and Software. New York, NY, USA: John Wiley and Sons.

Chen, D., Chen, R., Li, Y., and Tang, T. (2013). Online learning algorithms for train automatic stop control using precise location data of balises. *IEEE Transactions on Intelligent Transportation Systems*, 3(3), 1526–1535.

Faruqi, I., Waluya, M.B., Nazaruddin, Y.Y., and Tamba, T.A. (2018). Train localization using Unscented Kalman Filter-based sensor fusion. *International Journal of Sustainable Transportation Technology*, 1(2), 35–41.

Hansen, J.H.L., Takeda, K., Naik, S.M., Trivedi, M.M., Schmidt, G.U., and Chen, Y.J. (2016). Signal processing for smart vehicle technologies. *IEEE Signal Processing Magazine (Special Issue)*, 33(6).

Hansen, J.H.L., Takeda, K., Naik, S.M., Trivedi, M.M., Schmidt, G.U., and Chen, Y.J. (2017). Signal processing for smart vehicle technologies: Part 2. *IEEE Signal Processing Magazine (Special Issue)*, 34(2).

Julier, S. and Uhlmann, J. (2004). Unscented filtering and nonlinear estimation. *Proceedings of the IEEE*, 92(3), 401–422.

Julier, S. and Uhlmann, J. (1997). A new extension of the Kalman filter to nonlinear systems. In *Proc. AeroSense: 11th Int. Symp.Aerospace/Defense Sensing, Simulation and Controls, Orlando, FL, USA*.

Kuutti, S., Fallah, S., Katsaros, K., Dianati, M., Mccullough, F., and Mouzakitis, A. (2018). A survey of the state-of-the-art localization techniques and their potentials for autonomous vehicle applications. *IEEE Internet of Things Journal*, 5(2), 829–846.

Li, W. and Leung, H. (2003). Constrained unscented Kalman filter based fusion of GPS/INS/digital map for vehicle localization. In *Proceedings of the 2003 IEEE International Conference on Intelligent Transportation Systems, Shanghai, China*.

Lim, J.H., Yoo, W.J., Kim, L.W., Lee, Y.D., and Lee, H.K. (2018). Augmentation of GNSS by low-cost MEMS IMU, OBD-II, and digital altimeter for improved positioning in urban area. *Sensors*, 18(11).

Liu, C., Chen, W.H., and Andrews, J. (2010). Optimisation based control framework for autonomous vehicles: algorithm and experiment. In *Proceedings of the 2010 IEEE International Conference on Mechatronics and Automation, Xi'an, China*.

Lu, D., Cai, B., Wang, J., and Liu, J. (2019). Simulated-based GNSS for Maglev train localization performance analysis. In *Poceedings of the 2019 International Conference on Electromagnetics in Advanced Applications (ICEAA), Granada, Spain*.

Malvezzi, M., Vettori, G., Allotta, B., Pugi, L., Ridolfi, A., and Rindi, A. (2014). A localization algorithm for railway vehicles based on sensor fusion between tachometers and inertial measurement units. *Proceedings of the Institution of Mechanical Engineers, Part F: Journal of Rail and Rapid Transit*, 228(4), 431–448.

Meng, X., Wang, H., and Liu, B. (2017). A robust vehicle localization approach based on GNSS/IMU/DMI/LiDAR sensor fusion for autonomous vehicles. *Sensors*, 17(9).

Paden, B., Càp, M., Yong, S.Z., Yershov, D., and Frazzoli, E. (2016). A survey of motion planning and control techniques for self-driving urban vehicles. *IEEE Transactions on Intelligent Vehicles*, 1(1), 33–55.

Temple, W.G., Tran, B.A.N., Chen, B., Kalbarczyk, Z., and Sanders, W.H. (2017). On train automatic stop control using balises: Attacks and a software-only countermeasure. In *Proceedings of the 2017 IEEE 22nd Pacific Rim International Symposium on Dependable Computing (PRDC), Christchurch, New Zealand*.

Veillard, D., Mailly, F., and Fraisse, P. (2016). EKF-based state estimation for train localization. In *Proceedings of the 2016 IEEE SENSORS, Orlando, FL, USA*.

Zhou, J., Xiao, H., Jiang, W., Bai, W., and Liu, G. (2020). Automatic subway tunnel displacement monitoring using robotic total station. *Measurement*, 151.